Available online at www.sciencedirect.com

ScienceDirect

Solar Energy 115 (2015) 589–602

SOLAR ENERGY

www.elsevier.com/locate/solener

# Estimation of rooftop solar photovoltaic potential of a city

Rhythm Singh [a,b,*], Rangan Banerjee [b]

[a] National Institute of Construction Management and Research, 25/1 Balewadi, N.I.A. Post Office, Pune 411045, India
[b] Department of Energy Science and Engineering, Indian Institute of Technology Bombay, Powai, Mumbai 400 076, India

Received 1 November 2014; received in revised form 2 March 2015; accepted 9 March 2015
Available online 30 March 2015

Communicated by: Associate Editor Bibek Bandyopadhyay

**Abstract**

A methodology for estimating the rooftop solar photovoltaic potential for a region has been described. The methodology has been applied and illustrated for the Indian city of Mumbai (18.98°N, 72.83°E). It uses high-granularity land use data available in the public domain and GIS-based image analysis of sample satellite images to estimate values of the Building Footprint Area (BFA) Ratio. Photovoltaic-Available Roof Area (PVA) Ratio has been estimated by simulations in *PVSyst* and has been compared with relevant values from the literature. Solar irradiance (DNI and DHI) and ambient temperature data have been taken from Climate Design Data 2009 ASHRAE Handbook. Liu Jordan transposition model has been used for estimating the plane-of-array insolation. Effect of tilt angle on the plane-of-array insolation received has been studied to make an optimum choice for the tilt angle. Micro-level simulations in *PVSyst* have been used to estimate effective sunshine hours for the region of interest. The installed capacity, annual and daily generation profiles and capacity factor have been estimated for PV panels with different rated solar cell efficiency and power–temperature coefficient values.

The results show a potential of 2190 MW for Mumbai city with median efficiency panels, at an annual average capacity factor of 14.8%. Daily and monthly variation of the generation from the Rooftop PV Systems has been studied. Comparison with sample daily load profiles shows that large scale deployment of Rooftop Solar Photovoltaic Systems can provide 12.8–20% of the average daily demand and 31–60% of the morning peak demand for different months, even with median conversion efficiency panels. This method can be used to obtain the PV potential for any region.


*Keywords:* Rooftop Solar Photovoltaic Systems; Potential estimation; Land-use data; *PVSyst*

## 1. Introduction

Around 62.5% of the total area of India, i.e. around 2.0 million square kilometers, has an annual average Direct Normal Insolation of more than 5.0 kW h/m$^2$/day (India Solar Resource Maps, Solar Energy Centre, Ministry of New and Renewable Energy, Government of India, 2013). For most parts of the country, the built-up structures are low-height, having more horizontal spread. Thus there is likely to be a significant potential for rooftop solar photovoltaic electricity generation in India. The National Solar Mission of India (JNNSM) focuses mainly on MW-scale grid connected solar photovoltaic plants. There is a need to estimate and quantify the potential for rooftop solar photovoltaic in order to make a case for its large scale deployment. This paper develops and illustrates a method for estimating the rooftop solar photovoltaic potential for a large city like Mumbai.

There have been some studies for estimating the potential for solar photovoltaic power, in general, and rooftop photovoltaic power, in particular, in different regions around the

* Corresponding author at: National Institute of Construction Management and Research, 25/1 Balewadi, N.I.A. Post Office, Pune 411045, India. Tel.: +91 876 753 4185, +91 20 668 59302.
*E-mail addresses:* rsingh@nicmar.ac.in, rhythm@iitb.ac.in (R. Singh).

http://dx.doi.org/10.1016/j.solener.2015.03.016
0038-092X/

**Nomenclature**

| | |
|---|---|
| BFA | Building Footprint Area |
| PVA | Photovoltaic-Available Roof Area |
| JNNSM | Jawaharlal Nehru National Solar Mission |
| MCGM | Municipal Corporation of Greater Mumbai |
| ELU | Existing Land Use |
| QGIS | Quantum GIS |
| SPA | Special Planning Authority |
| $D_b$ | Building Density |
| $D_p$ | Population Density |
| $E_{PV}$ | energy output of a PV panel in an hour |
| $E_{sol}$ | energy incident on unit area of a PV panel in an hour |
| $\eta_{pv}$ | rated efficiency of a PV panel |
| $\eta_{pcu}$ | efficiency of power conditioning unit including inverter |
| PTC | Power Temperature Coefficient |
| NOCT | Nominal Operating Cell Temperature |
| POA | Plane of Array |
| TOD | Time-of-Day |
| MPP | Morning Partial Peak |
| MP | Morning Peak |
| APP | Afternoon Partial Peak |

globe, using different models and methodologies. Izquierdo et al. (2008) proposed a method for estimating the geographical distribution of rooftop areas available for solar PV installation in the provinces of Spain, in order to estimate the overall potential for large scale deployment of the technology. It is based on land uses, population and building densities data and on a "statistically representative stratified-sample of vectorial GIS maps of urban areas." Thus they estimated the total and per capita available area on roofs of Spain for photovoltaic installations. Ordóñez et al. (2010) analyzed the grid-connected solar photovoltaic capacity of residential rooftops in the Andalusia province of Spain. For this they used a description of building characteristics leading to the calculation of the roof area where photovoltaic systems can be installed. Wiginton et al. (2010) used geographic information systems and object-specific image recognition "to determine the available rooftop area for PV deployment in an example large-scale region in south eastern Ontario". They estimated that around 30% of Ontario's energy needs can be met with electricity generated from rooftop photovoltaic systems. Bergamasco and Asinari (2011) developed a methodology for estimation of photovoltaic solar energy potential of rooftops in the Piedmont region in north-western Italy. The roof area suitable for this application is estimated from analysis of GIS data, and different strategies for solar energy exploitation have been proposed and analyzed. Jakubiec and Reinhart (2012) used a combination of LiDAR measurements, GIS data and DAYSIM simulations on an hourly basis for estimation of urban rooftop photovoltaic potential. They applied this methodology to the city of Cambridge, Massachusetts, USA containing over 17,000 buildings. Rooftop Revolution (Greenpeace India, 2013) is the only study assessing the rooftop solar photovoltaic potential of any region in India, done by Greenpeace and Bridge to India for the National Capital Territory of Delhi. They have used data from government agencies and online mapping tools as inputs. The analysis is, however, based mostly on thumb-rules, standard assumptions and experts' opinions.

The methods used in the above studies, except (Greenpeace India, 2013), cannot be applied as it is to Indian situations, due to data unavailability; whereas, (Greenpeace India, 2013) is based more on thumb-rules and lacks methodological rigor.

This paper proposes a hybrid methodology for estimating the rooftop solar photovoltaic potential of Mumbai which is based on micro–macro synthesis and uses public-domain secondary data. The methodology suits the data availability for the concerned region and ensures proper methodological rigor. It draws upon the public-domain high granularity Land Use data provided by a government agency; uses micro-simulations in *PVSyst* and geo-spatial image analysis of satellite imagery of the concerned area, along with analysis of parametric values from the literature to determine the rooftop photovoltaic potential. This particular approach has the advantage of micro–macro synthesis and has not been used before for estimating the land resource availability for potential estimation. The simultaneous implementation of these diverse strategies helps overcome the limitations that arise due to unavailability of data. For radiation transposition models, a suitable choice for the location of interest has been made by analyzing findings from the literature. A relevant scenario for large scale rooftop solar photovoltaic installation has been developed, based on appropriate system design parameters.

## 2. Methodology

The methodology has been represented graphically in the block diagram in Fig. 1. It has been illustrated for the municipal city limits of Mumbai (MCGM).

The main blocks in this block diagram are:

(i) Area Estimation Block.
(ii) Insolation Estimation Block.
(iii) PV Device & System Block.
(iv) Results and Analysis Block.

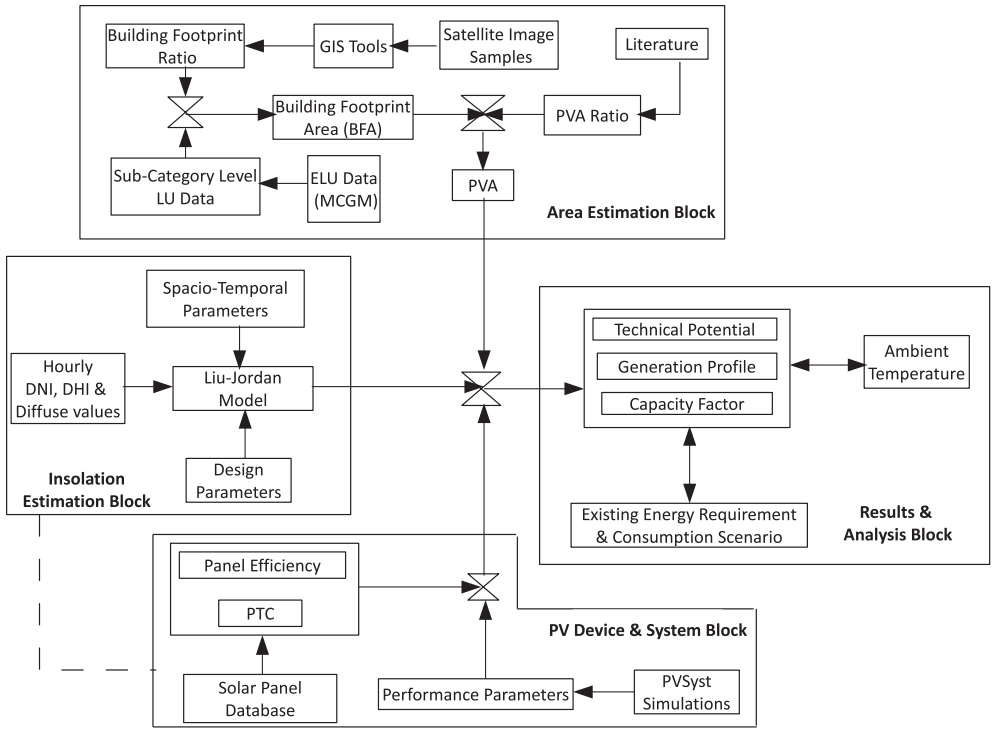


Fig. 1. Block diagram of the proposed methodology.

Table 1
Samples for GIS-based analysis.

| S. no. | Land Use Type | Samples taken from ward # | Samples/ward | Total number of samples |
|---|---|---|---|---|
| 1 | Residential | A, D, F/N, G/S, H/W, K/W, M/E, P/N, R/C, T | 3 | 30 |
| 2 | Commercial | A, B, C, E, F/S, K/E, P/S | 3 | 21 |
| 3 | Industrial | E, G/S, L, M/E, M/W, N, S | 3 | 21 |
| 4 | Office | A, E, F/N, G/S, P/S | 3 | 15 |
| 5 | Medical Amenities | A, D, E, F/N, F/S | 2 | 10 |
| 6 | Social Amenities | A, B, C, G/S, M/E | 2 | 10 |
| 7 | Educational Amenities | A, B, F/N, F/S, H/E, K/E, N, P/S, R/N, S | 1 | 10 |
| 8 | Railway Station | B, D, E, F/N, F/S, G/S, H/W, K/E, K/W, M/E, P/N, P/S, R/C, S, T | 1 | 15 |
| 9 | Telephone Exch./P&T Office | A, G/N, H/W, K/E, R/C | 1 | 5 |
| 10 | Railway Terminal | A, G/N, L, N | 1 | 4 |
| 11 | Building Public Parking | D, K/W, S | 1 | 3 |

The detailed description of each of these blocks follows. The list of parameters used as inputs for the methodology and the sources for their values has been compiled in Appendix A.

### 2.1. Area estimation block

This block is meant for estimation of the total rooftop area available for installation of solar photovoltaic systems and the total active solar photovoltaic area in the region of interest.

The Municipal Corporation of Greater Mumbai (MCGM) is the primary agency responsible for urban governance in Mumbai city. The total area under the administration of MCGM is 458.27 sq. km, inhabiting a population of 12.5 million (2011) (Mumbai (Greater Mumbai) Metropolitan Urban Region Population 2011 Census, 2011).

This methodology takes into account detailed categorization and sub-categorization of the land-use types. The Existing Land Use (ELU) data for Mumbai city, provided by MCGM, is used for this purpose (Existing Land Use Survey for Development Plan for Greater Mumbai (2014–2034), 2014). The municipal area of MCGM has been classified into 24 wards, numbered from A to T (some wards are divided into two – like F/North and F/South,

Table 2
Building footprint ratio of relevant land use categories and sub-categories.

| S.No. | Land Use Type | Permissible Categories | Permissible Sub Category | Mean Building Footprint Ratio |
|---|---|---|---|---|
| 1 | Residential | | | |
| | | a) Individual Housing | ALL | 0.75 |
| | | b) Apartments/ Multifamily | ALL | 0.5 |
| | | c) Government / Municipal Staff / Quarters / Housing | ALL | |
| 2 | Commercial | | | |
| | | a) Hotels | I. Star Category | 0.5 |
| | | | II. Others | 0.75 |
| | | b) Retail Markets | I. Municipal Market | 0.55 |
| | | | II. Shopping Centre | |
| | | | III. Mall | 0.75 |
| | | c) Storages & Warehouses | ALL | 0.9 |
| 3 | Offices | ALL | ALL | 0.75 |
| 4 | Educational Amenities | | | |
| | | a) Schools | ALL | 0.45 |
| | | b) Colleges except University/IIT | ALL | 0.3 |
| | | c) University/IIT | -- | 0.1 |
| 5 | Medical Amenities | | | |
| | | a) Hospital | ALL | 0.55 |
| | | b) Maternity Home | -- | |
| | | c) Dispensary | ALL | |
| 6 | Social Amenities | | | |
| | | a) Welfare Activities | I. Public Hall | 0.5 |
| | | b) Entertainment Centers | I. Auditorium / Theater | |
| | | | II. Cinema /Multiplex | |
| | | c) Recreational Activities | I. Art Gallery | |
| | | | II. Museum | |
| | | d) Law & Order | I. Police Station | 0.3 |
| | | | II. Court | |
| | | | III. Prison | |
| | | e) Public Sanitary Convenience | -- | 0.75 |
| 7 | Transport and Communication | | | |
| | | a) Transport | I. Building Public Parking | 0.9 |
| | | | II. Railway Stations | 0.45 |
| | | | III. Railway Terminal | 0.4 |
| | | b) Communication | I. Post and Telegraph Office | 0.75 |
| | | | II. Telephone Exchange | |
| 8 | Industrial Use | ALL | ALL | 0.3 |

etc.). The ELU data provided by the MCGM gives the detailed land use analysis for each of these wards. The complete area of each ward has been classified into broad Land Use Types like Residential, Commercial, Industrial, Offices, Educational Amenities, etc. Within each Type, there are several Land Use Categories like, for example, in the Residential Type, there are Categories as Individual Housing, Apartment, Government Housing, Slums, etc. Further, each Land Use Category has been divided into finer Sub-Categories like, for example, the

Sub-Categories in the Individual Housing Category are "Primary Residential Zone_Individual Housing" and "Individual Housing with Commercial". The exact land area used under each Sub-Category has been provided by MCGM. There are a total of 14 Land Use Types, 38 Land Use Categories and 145 Sub-Categories of Land Use in the classification done by MCGM.

However, not all the Land Use Categories and Sub-Categories can provide building structures suitable for installation of Rooftop Solar Photovoltaic Systems. A conservative approach has been adopted, and only those Land Use Categories and Sub-Categories have been chosen which are likely to have rigid built-up structures with the requisite structural stability and permanence to be able to support the installation of Rooftop Solar Photovoltaic Systems. Based on this criterion, the Land Use Categories and Sub-Categories that have been found to be suitable for installation of Rooftop Solar Photovoltaic Systems have been indicated in Table 2.

### 2.1.1. Estimation of Building Footprint Area (BFA) Ratio

For each of the above mentioned categories and/or sub-categories the BFA Ratio is to be determined, i.e. the ratio of the actual area covered by the building to the plot area of the building.

$$\text{BFA Ratio} = \frac{A_{\text{built}}}{A_{\text{plot}}} \tag{1}$$

where $A_{\text{built}}$ is the actual area covered by a built-up structure, and $A_{\text{plot}}$ is the plot area of the building. At a gross level, say ward-level or city-level, BFA Ratio can be defined as

$$\text{BFA Ratio (Aggregate)} = \frac{\sum A_{\text{built}}}{\sum A_{\text{plot}}} \tag{2}$$

This is needed because the ELU data gives the area on ground used for different land uses, but it does not measure how much of that area is used for the actual building on that premises.

For estimating this, we have taken random image samples of few buildings of each relevant Land Use Type, the details of which are given in Table 1.

The actual area covered by the built-up structure and the area of the premises demarcated for the building have been estimated using satellite imagery and GIS packages, for each of the samples.

Fig. 2 shows a section of the ELU map of Ward A of MCGM, provided by the MCGM in its ELU Report. Fig. 3 shows the satellite image corresponding to the highlighted segment of the ELU map (inside the black-bordered square). This was used as a sample for residential buildings from Ward A. This satellite image is from Google Earth™, obtained from GeoEye's GE-1 satellite, having a spatial resolution of 0.5 m.

The satellite image is georeferenced using the Georeferencer plug-in of Quantum GIS (QGIS) 1.8.0. The Coordinate reference system used for georeferencing is WGS84, and the transformation type is linear. Though the minimum number of control points needed for this transformation type is three, to ensure greater accuracy, five control points have been taken for each image. The Area Measurement functionality of QGIS has been used for calculating the areas relevant to the estimation of the BFA Ratio. The results of the estimation procedure, rounded to the nearest multiple of 0.05, have been shown in Table 2.

### 2.1.2. Estimation of Total Building Footprint Area (BFA) under MCGM

In the '*w*' municipal wards of Mumbai (MCGM) '*s*' Land Use Sub-Categories have been identified to have

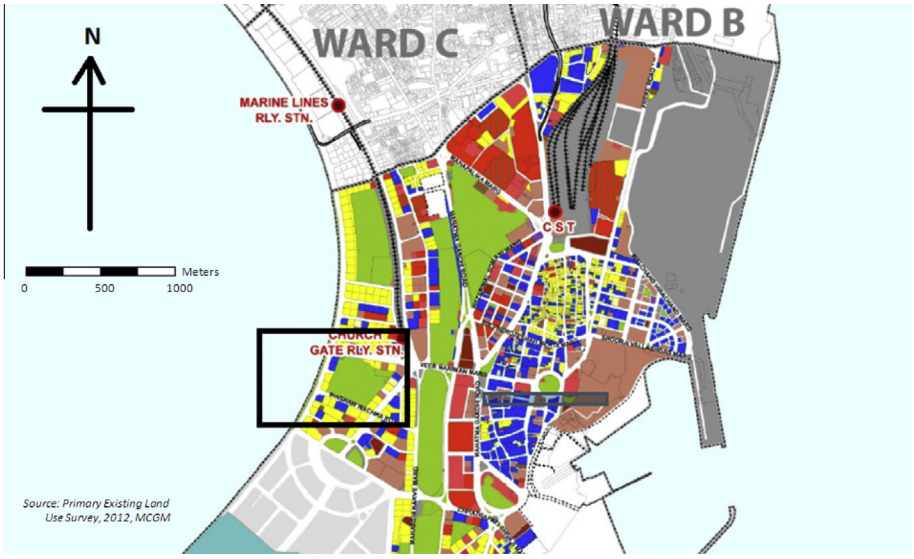


Fig. 2. A section of ELU map of Ward A of MCGM with the sample area highlighted.

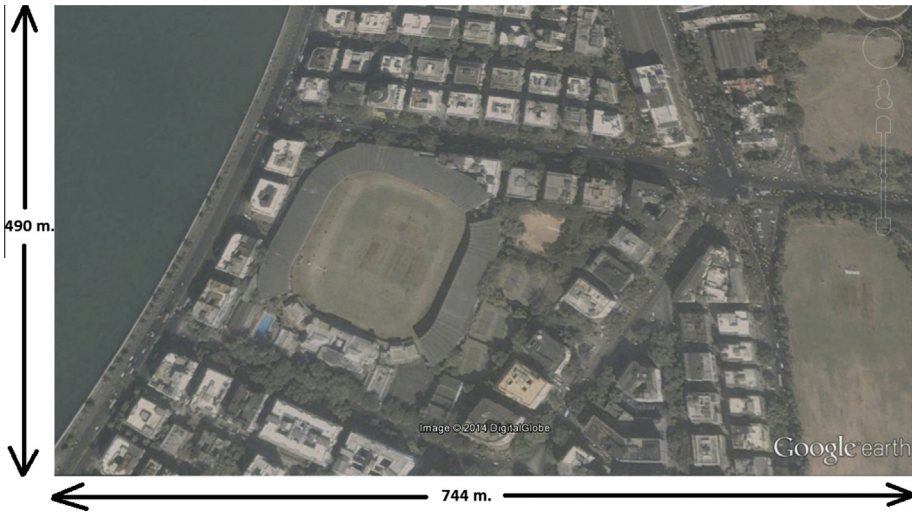


Fig. 3. Satellite Imagery of the sample area highlighted in Fig. 2, from Google Earth™.

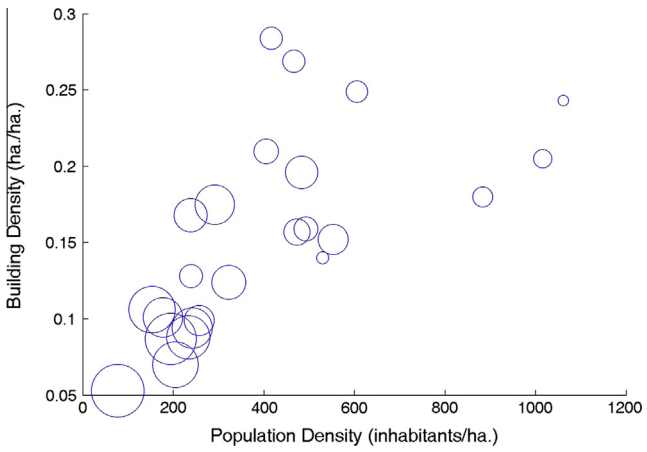


Fig. 4. Building Density vs. Population Density (circle sizes proportionate to Ward Area).

buildings suitable for the installation of Rooftop Photovoltaic Systems. The Building Footprint Ratio for each of these Land Use Sub-Categories has been estimated. Building Footprint Ratio of the $i$th Land Use Sub-Category is denoted by $b_i$. Also, the area used for the $i$th Land Use Sub-Category in the $j$th ward is denoted as $A_{ij}$. Thus the total Building Footprint Area is given by:

$$\mathrm{BFA} = \sum_{j=1}^{w}\sum_{i=1}^{s} A_{ij} \cdot b_i \tag{3}$$

Using the above formula, the total Building Footprint Area under all the MCGM wards has been estimated. Building Density ($D_b$) for each ward, and for the whole of MCGM, has also been estimated. It is used for estimating the BFA for Special Planning Authority (SPA) areas falling within the municipal limits of MCGM, as these are not covered in the ELU survey of MCGM. Building Density ($D_b$) is defined as

$$D_b = \frac{\mathrm{BFA}}{\text{Total area (TA)}} \tag{4}$$

Population Density ($D_p$) (population estimates taken from Mumbai (Greater Mumbai) Metropolitan Urban Region Population 2011 Census (2011)) has been estimated for each ward of MCGM and for the whole of MCGM, which has been defined as

$$D_p = \frac{\text{No. of inhabitants}}{\text{Area (hectares)}} \tag{5}$$

The graph in Fig. 4 shows the variation of Building Density and Population Density across the wards of MCGM.

### 2.1.3. Estimation of BFA for areas under Special Planning Authority (SPA) within municipal limits of Mumbai

There are certain pockets within the municipal limits of Mumbai which have been demarcated as coming under the authority of Special Planning Authority (SPA). The ELU survey of MCGM, and hence the ELU maps and reports provided by MCGM, do not cover these areas. The total area of each SPA area is known, but data regarding land-use categories and sub-categories is unavailable. Thus in order to estimate the Building Footprint Area of the SPA areas, there is a need to correlate each SPA area to the wards of MCGM, detailed land-use data for which are available.

The dominant land use pattern is known for each SPA area. Based on the major Land Use Type, each SPA area has a characteristic Building Density profile. We correlate the dominant Land Use Type of each of these SPA areas to that of one (or more) of the 24 MCGM wards. Accordingly, each SPA area is assigned a $D_b$ value characterizing its Building Density profile, which is mean of the $D_b$ values of those MCGM wards which have a land use pattern similar to the SPA area in consideration. The resultant $D_b$ values for each of the SPA areas and the Building

Table 3
$D_b$ and BFA values for the SPA Areas.

| S. no | Authority | Area (ha.) | Usage | Correlation to MCGM wards | Resultant $D_b$ | BFA (ha) |
|---|---|---|---|---|---|---|
| 1 | SPA (Back Bay Reclamation) | 236.94 | Mainly Office Area | Ave. of highest 6 (Top 25%ile) | 0.243 | 57.66 |
| 2 | SPA (Wadala Truck Terminal Area) | 119.87 | Truck Terminal | Ave. of lowest 6 (Bottom 25%ile) | 0.082 | 9.80 |
| 3 | SPA (Dharavi) | 234.37 | Mainly Slum Area | – | 0 | 0 |
| 4 | SPA (Bandra Kurla Complex) | 638.84 | Mainly Office Area | Ave. of middle 12 (Middle 50%ile) | 0.149 | 95.12 |
| 5 | SPA MMRDA | 19.57 | General | Ave. of all | 0.156 | 3.05 |
| 6 | International Airport | 836.02 | Airport | As per CSIA Development Plan | 0.063 | 52.67 |
| 7 | MIDC | 130.95 | Mainly Industrial Area | Ave. of middle 12 (Middle 50%ile) | 0.149 | 19.50 |
| 8 | SPA (Oshiwara District Center) | 99.22 | General | Ave. of all | 0.156 | 15.45 |
| 9 | SPA (Recreation and Tourism Development Zone) | 2006.99 | Mainly Green Area | – | 0 | 0 |
| | Area in Mumbai Outside MCGM (ha) | 4322.77 | | | | 253.25 |

Table 4
Sector-wise BFA Ratio results & comparison with literature.

| S. no. | Sector | Mumbai (this paper) | Taiwan (Yue and Huang, 2011) |
|---|---|---|---|
| 1 | Residential | 0.52 | 0.58 |
| 2 | Commercial | 0.72 | 0.66 |
| 3 | Offices | 0.75 | 0.5 |
| 4 | Education | 0.31 | 0.27 |
| 5 | Health | 0.5 | 0.3 |
| 6 | Social & Civic Amenities | 0.48 | 0.47 |
| 7 | Transport | 0.5 | – |
| 8 | Industry | 0.3 | 0.63 |

Table 5
Characteristics of the ward-level BFA Ratio (aggregate).

| Characteristic | Mumbai (this paper) | Spain (Izquierdo et al., 2008) |
|---|---|---|
| Range | 0.353–0.579 | 0.46–0.88 |
| Mean | 0.481 | 0.572 |
| Std. Dev. | 0.056 | 0.121 |

Footprint Area for each SPA area, as well as the total has been shown in Table 3.

### 2.1.4. Analysis of the BFA Ratio results

The BFA Ratios estimated above have been aggregated with respect to the different Land Use Types and Sectors. Yue and Huang (2011) did similar analysis for 7 cities and 15 counties of Taiwan. Table 4 shows the sector-wise results for our case and comparison with the results of Yue & Huang.

If we consider only those Land Uses which can support Rooftop PV (Table 2), then the aggregate characteristics of the BFA Ratio values for the 24 Wards of MCGM have been shown in Table 5. Table 5 also shows the results for a comparable analysis done by Izquierdo et al. (2008) for the 3086 urban municipalities of Spain.

The results obtained by Izquierdo et al. (2008) show a larger range and a larger standard deviation from the mean, as compared to the Mumbai results, because they have covered 3086 urban municipalities in Spain, as opposed to a single city.

### 2.1.5. Estimation of PVA from BFA

To obtain the Effective Photovoltaic-Available Roof Area (PVA) for all the rooftops in the city of Mumbai, from the total BFA, a ratio called PVA Ratio has been defined. PVA Ratio is defined as the ratio of the effective area of solar photovoltaic panels installed on the rooftop of a building(s) to the total Building Footprint Area of the building(s).

$$\text{PVA Ratio} = \frac{\text{PVA}}{\text{BFA}} \tag{6}$$

The PVA Ratio needs to be defined because the complete rooftop area cannot be fully used for installation of photovoltaic systems. There, invariably, is a loss of rooftop area vis-à-vis area suitable for PV installation, due to several factors. The prominent ones are:

(i) Shading, due to the neighboring structures, trees or, sometimes, other parts of the roof itself.

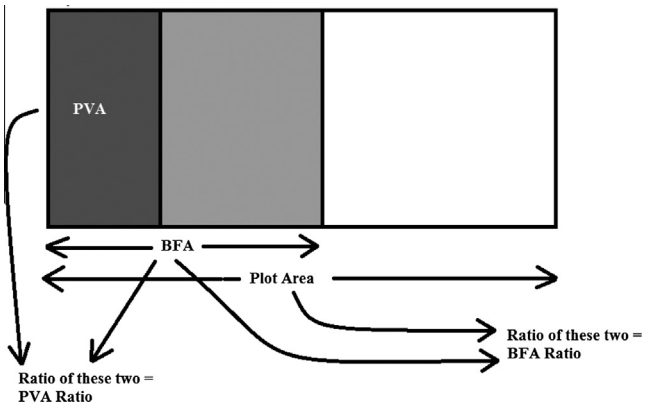


Fig. 5. Correlation between PVA, BFA and Plot Area.

Table 6
Values of PVA Ratio from literature.

| S. no. | Researcher | Year | Area Covered | PVA Ratio | Comments |
|---|---|---|---|---|---|
| 1 | IEA BIPV Report (International Energy Agency, 2002) | 2002 | Global | 0.4 | |
| 2 | Scartezzini et al. (2002), Montavon et al. (2004) | 2002, 2004 | Switzerland | 0.49–0.95 | Mean = 0.723 |
| 3 | Pillai and Banerjee (2007) | 2007 | India | 0.3 | |
| 4 | Izquierdo et al. (2008) | 2008 | Spain | 0.22–0.43 | Mean = 0.346 |
| 5 | Ordóñez et al. (2010) | 2010 | Andalusia, Spain | 0.535 | For Flat Roof |
| 6 | Wiginton et al. (2010) | 2010 | Ontario, Canada | 0.3 | |
| 7 | Bergamasco and Asinari (2011) | 2011 | Italy | 0.145, 0.405 | Residential, Industrial |
| 8 | Yue and Huang (2011) | 2011 | Taiwan | 0.4 – 0.5 | Mean = 0.45 |
| 9 | Theodoridou et al. (2012) | 2012 | Thessaloniki, Greece | 0.146 | |
| 10 | Karteris et al. (2013) | 2013 | Greece | 0.25 | |
| 11 | Rooftop Revolution (Greenpeace India, 2013) | 2013 | Delhi, India | 0.26 | |

Table 7
Area Estimation Results' Summary.

| S. no. | Specification | Area (ha.) |
|---|---|---|
| 1 | Total area under MCGM administration | 41,506 |
| 2 | Total area under SPAs within MCGM limits | 4323 |
| *Taking in account the BFA Ratios for all the sub categories and SPAs* | | |
| 3 | Total BFA under MCGM administration | 5141 |
| 4 | Total BFA under SPAs within MCGM limits | 253 |
| 5 | Total BFA for Mumbai | 5394 |
| *Taking PVA Ratio for Mumbai as 0.28* | | |
| 6 | Total PVA Area for Mumbai | 1510 |

(ii) The use of roof area for other purposes, and/or the utilities installed on the roof.
(iii) The limitations imposed due to the irregularity of the roof area, due to which some portions of the roof are not suitable for the installation and racking of the PV systems.

In some cold climate countries there is an additional problem of inclined roofs and/or pitched roofs. However, this is hardly encountered in practical Indian settlements, and hence, has not been considered.

The correlation between PVA, BFA and Plot Area has been shown in Fig. 5. It is a representational schematic and not to any scale. Table 6 lists the values of fraction of roof area available for solar photovoltaic/solar thermal installations used by different researchers for different regions of study.

To ascertain the PVA ratio for our analysis, we have done simulations for some sample buildings of residential, commercial, office and educational Land Use Types in *PVSyst*. The PVA ratio values for these sample buildings from Mumbai lies in the range 0.28–0.4. Taking a conservative approach, we have adopted a value of 0.28 for this work. As can be seen from Table 6, this is a quite conservative value as far as similar values for this factor from literature are concerned. Also, interestingly, this is equal to the mean of the only two literature values for this factor for India.

#### 2.1.6. Summary of Area Estimation Results

The overall results for estimation of Photovoltaic-Available Rooftop Area for the city of Mumbai (MCGM) have been summarized in Table 7.

### 2.2. Insolation Estimation Block

This block is meant to estimate the effective plane-of-array (POA) insolation for the rooftop PV system and other system design parameters like tilt, etc.

#### 2.2.1. Transposition Model

Photovoltaic Systems make use of not only the Direct Normal Irradiance (DNI) but also the Diffuse Horizontal Irradiance (DHI). The transposition model should be able to account not only for both the DNI and the DHI, but also for the ground-reflected irradiance, along with the system-design parameters, such as array orientation, tilt, and tracking, if applicable.

Liu-Jordan model (Liu and Jordan, 1960) has been chosen for estimating all the POA irradiances in our calculations, due to the following advantages (Evseev and Kudish, 2009; Bilbao et al., 2003; Kambezidis et al., 1994; Gueymard, 2009; Notton et al., 2006; Padovan and Del Col, 2010; Demain et al., 2013):

1. It is the simplest of all the transposition models and has very less data-intensity and calculation-complexity.
2. RMSE% ranges from 8.5% to 19.4%, at a 1-h time-step, for a wide range of latitude and tilt angle values.
3. Takes into account not only the DNI and DHI values, but also the ground-reflected irradiance.
4. Does not consider horizon-brightening effects, reducing the risk of overstating the true POA irradiance.

The mathematical representation of the Liu-Jordan model is given in Eq. (7).

$$I_t = I_N \cos\theta_i + I_d \frac{1+\cos\beta}{2} + \rho(I_N \cos\theta_z + I_d) \times \frac{1-\cos\beta}{2} \quad (7)$$

Table 8
Parametric inputs to the transposition model.

| S. no. | Parameter | Value | Justification |
|---|---|---|---|
| 1 | Wall Azimuth angle ($\gamma_{wall}$) | 0° | Flat rooftops. Assumption that all panels are oriented S-facing (for maximizing POA irradiance in general). (General assumption in absence of individual optimization for each roof.) |
| 2 | Hour angle ($\omega$) | Calculated for 0600–2000 h | Possible range of sunshine hours |
| 3 | Albedo ($\rho$) | 0.2 | Standard value for urban surroundings |
| 4 | Latitude ($\phi$) | 18.98° | |
| 5 | Tilt of the PV array ($\beta$) | 19° | Given in Section 2.2.3 |
| 6 | Solar declination ($\delta$) | Calculated for all the days of a year, from $n = 1$ to 365; averaged on monthly basis | Solar irradiance data available is the monthly mean of irradiance values of each hour |
| 7 | Angle of incidence ($\theta_i$) | Calculated for each day on hourly basis, averaged on monthly basis | |
| 8 | Zenith angle ($\theta_z$) | -do- | |

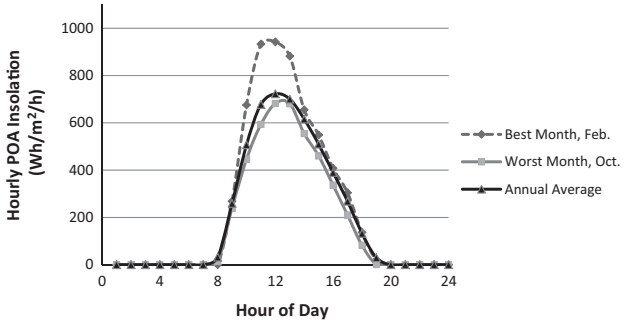


Fig. 6. Fixed Tilt @ 19°: POA solar radiation for Mumbai.

where the symbols used have their usual meanings.

Table 8 summarizes the values for the parametric inputs to this model. Using all these parameters and the input values of monthly mean DNI and DHI values for each hour, as mentioned before, the monthly mean POA irradiance values for each hour have been calculated.

### 2.2.2. Solar Insolation Data

Solar Insolation Data for all the calculations have been taken from Climate Design Data 2009 ASHRAE Handbook (American Society of Heating, Refrigerating and Air Conditioning Engineers, 2009). These data have been generated from a period of record of around 30 years.

The relevant data for this work are Direct Normal Insolation, Diffuse Horizontal Insolation and Global Horizontal Insolation. Each of these has been provided in the form of monthly mean solar insolation for each hour of the day. The average hourly statistics for dry bulb temperatures have also been used for estimating the impact of temperature on the output derived from the photovoltaic system.

### 2.2.3. Design parameters

The impact of tilt angle on solar photovoltaic generation has been analyzed for a range of values of tilt angle. The results for Annual Average POA Insolation, calculated as per Liu–Jordan Model, shows that the year-round optimal tilt angle for PV planes in Mumbai (18.98°N, 72.83°E) is 19°. Hence fixed tilt at 19° has been chosen as the base case for our analysis. The POA solar radiation profiles for this scenario, for the month with highest average daily insolation, month with lowest average daily insolation and the annual average are shown in Fig. 6.

### 2.2.4. Estimation of the effective sunshine hours

Due to the rooftop solar photovoltaic system's being situated at a height, sunlight is not incident on it for a fraction of an hour during early morning (just after sunrise) and late afternoon (just before sunset). The effective sunshine hours, during which the rooftop photovoltaic system produces electricity, have been estimated by simulations in *PVSyst* for different building heights. The monthly mean POA solar insolation values calculated by Eq. (7) have been accordingly adjusted to represent only the insolation during the effective sunshine hours, for each month. This results in a 3.2% decrease in the annual average POA insolation.

## 2.3. PV Device & System Block

This block analyzes the impact of choice of different PV devices, along with the system parameters, on the output obtained in the scenario detailed so far. Ambient temperature effects have also been taken into consideration. Average capacity factor has been calculated for each month.

### 2.3.1. Expected output from the Rooftop PV Systems

The electrical energy output from a solar photovoltaic panel is given by Eq. (8).

$$E_{PV}\ (\text{kW h}) = E_{sol}\ (\text{kW h/m}^2) \times A\ (\text{m}^2) \times \eta_{PV} \times \eta_{PCU} \tag{8}$$

where $E_{PV}$ is the energy output of the solar PV panel in an hour and $E_{sol}$ is the incident solar energy, in an hour, on a unit area; $A$ is the area of the panel; $\eta_{pv}$ is the rated efficiency of the PV panel; $\eta_{pcu}$ is the efficiency of the power conditioning unit including the inverter. For the present analysis, monthly mean hourly solar insolation values are

used. Therefore the estimation for generation from the rooftop solar photovoltaic system is carried out on an hourly basis, for a typical day from each month of the year. Thus, Eq. (8) gets modified to Eq. (9).

$$\sum_{N_{sh}} E_{PV}\ (\mathrm{kW\,h}) = \sum_{N_{sh}} E_{sol}\ (\mathrm{kW\,h/m^2}) \times A\ (\mathrm{m^2}) \times \eta_{PV} \times \eta_{PCU} \tag{9}$$

where $N_{sh}$ is the number of effective sunshine hours.

SRoeCo Solar (2013) gives a comprehensive database of commercially available solar panels. This database was accessed in October, 2013–January, 2014 and a total of 12,622 entries for solar panels of different materials, made by different companies, with different conversion efficiencies had been found. For estimating the base case, the panel having the rated Median Efficiency of the database, which has been found to be 14.5% ($\eta_{pv}$), has been chosen.

However, this is the theoretical/rated value of the solar panel efficiency. In actual practice, the efficiency varies due to the impact of the ambient temperature. The ratings of a PV panel are defined under Standard Test Conditions (STC), viz. 1000 W/m$^2$ solar irradiation and 25 °C panel temperature. The effect of temperature is quantified by a quantity known as the Power Temperature Coefficient (PTC), defined as the percentage change in the output of a PV panel for every degree Celsius of temperature variation from the standard 25 °C temperature of the PV panel. The value of PTC is negative for the solar cell materials, and hence the efficiency decreases with increase in temperature beyond 25 °C. Hence, Eq. (9) gets modified to

$$\sum_{N_{sh}} E_{PV}\ (\mathrm{kW\,h}) = \sum_{N_{sh}} \left( E_{sol}\ (\mathrm{kW\,h/m^2}) \times A\ (\mathrm{m^2}) \times \eta_{PV} \times \left(1 + \frac{\mathrm{PTC} \times \left(T_{panel,h}\ (^\circ\mathrm{C}) - 25\right)}{100}\right) \times \eta_{PCU} \right) \tag{10}$$

where $T_{panel,h}$ is the monthly mean panel temperature during the $h$th hour, which is estimated by Eq. (11) (Rose, 1980).

$$T_{panel,h}\ (^\circ\mathrm{C}) = T_{Air,h}\ (^\circ\mathrm{C}) + \frac{\mathrm{NOCT} - 20}{800} E_{sol}\ (\mathrm{W/m^2}) \tag{11}$$

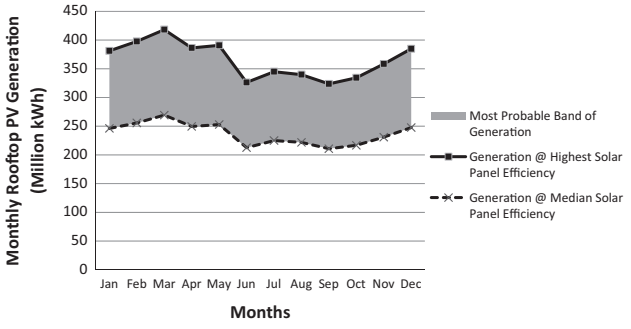


Fig. 7. Variation in generation with solar panel efficiency.

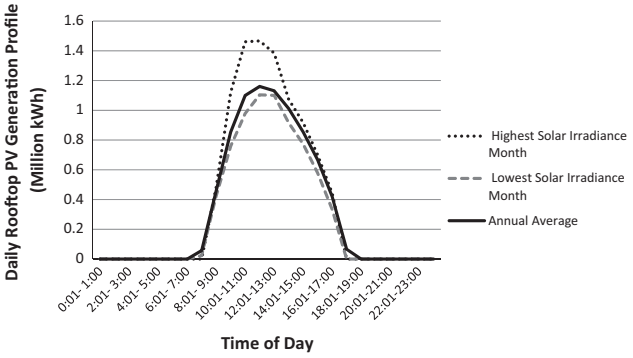


Fig. 8. Typical daily generation profiles for Mumbai.

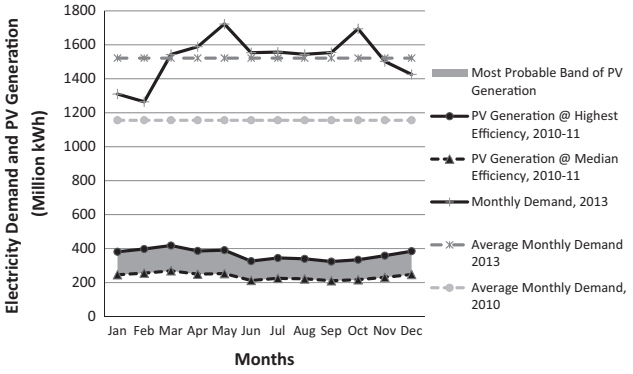


Fig. 9. Comparison with existing power scenario.

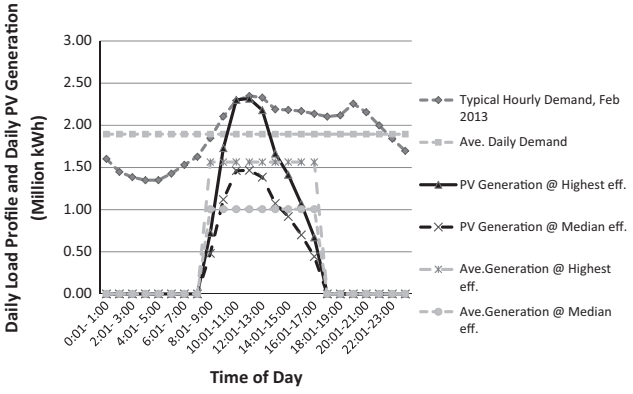


Fig. 10. Typical Load Profile vs PV generation (highest mean daily insolation): Feb., 2013.

$T_{Air,h}$ is the monthly mean ambient temperature during the $h$th hour, which has been taken from the database referred to in Section 2.2.2; $E_{sol}$ is same as defined above and Nominal Operating Cell Temperature (NOCT) is defined as the temperature reached by open circuited cells in a module under the following conditions: irradiance on cell surface = 800 W/m$^2$; Air temperature = 20 °C; wind velocity = 1 m/s, with open back side mounting. Ross and Smokler (1986) report the NOCT for an average solar panel operating in typical conditions to be around 48 °C.

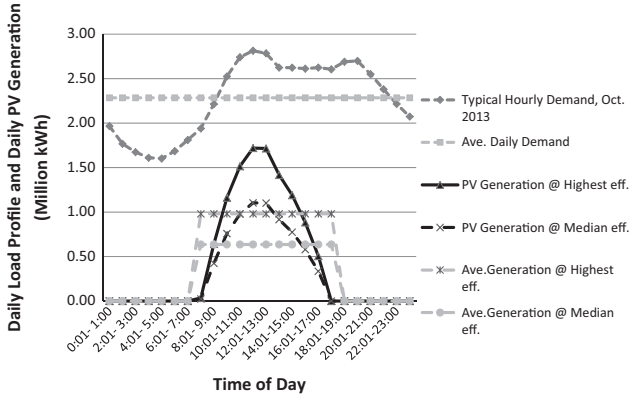


Fig. 11. Typical Load Profile vs PV generation (lowest mean daily insolation): Oct., 2013.

Eq. (10) is finally used for estimation of the rooftop photovoltaic electricity generation.

For estimating the efficiency of the power conditioning unit including the inverter, simulations have been carried out in *PVSyst*, considering a typical system with 175Wp, 30 V, polycrystalline Si modules of BP Solar (BP 4175 N) and a 60 kW, 405–750 V, 50/60 Hz Ingecon Sun 60 Inverter. Based on the results, we have used a value of 85% for $\eta_{pcu}$ for our output analysis.

In order to put the rooftop PV generation scenario in perspective of other options, capacity factor has also been evaluated. Capacity factor is defined as the ratio of the electrical energy output obtained from a plant to the maximum possible energy output possible from the plant.

$$\text{Capacity factor} = \frac{E_{out}\ (\text{kW h})}{\text{IC}\ (\text{kW}) \times 365 \times 24} \tag{12}$$

where $E_{out}$ is the actual annual energy output from the plant and IC is the rated installed capacity.

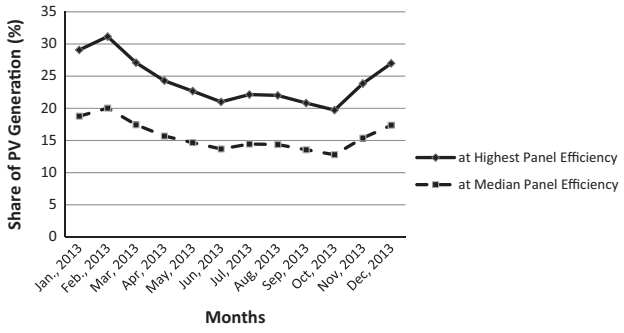


Fig. 12. Generation from PV as % of daily demand.

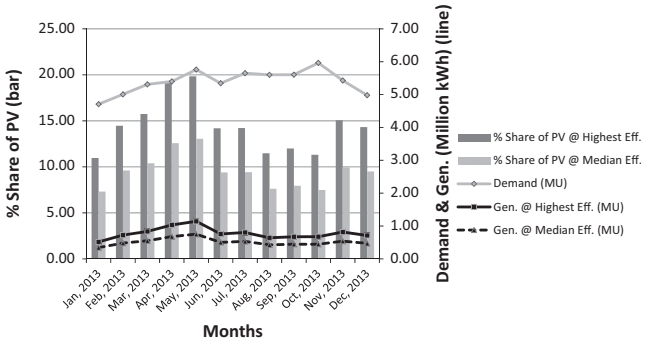


Fig. 13. Demand, generation from PV and % share of demand: Morning Partial Peak (MPP).

### 2.3.2. Parametric variation

The two rated panel efficiencies – 21.57% (SunPowerSPR-X21-255, 255Wp rated) and 14.5% (Tata Power Solar SystemsTP285LBZ, 285Wp rated) – which are the highest commercial solar panel efficiency and the median solar panel efficiency of the database in SRoeCo Solar: Solar Panel Comparison Table (2013) – represent

Table 9
Comparison of Typical Solar PV Generation with Typical Load Profiles.

| S. no | Month, year | Mean Daily Demand (Million kW h) | Typical Day | Typical No. of Eff. Sunshine Hours ($N_{sh}$) | Typical Daily PV Generation (Million kWh) | | PV as % of Daily Demand | |
|---|---|---|---|---|---|---|---|---|
| | | | | | @ Highest Eff. | @ Median Eff. | @ Highest Eff. | @ Median Eff. |
| 1 | January, 2013 | 42.27 | 21/01/13 | 8.67 | 12.29 | 7.94 | 29.08 | 18.78 |
| 2 | February, 2013 | 45.18 | 23/02/13 | 9.17 | 14.08 | 9.05 | 31.15 | 20.03 |
| 3 | March, 2013 | 49.78 | 04/03/13 | 9.75 | 13.49 | 8.69 | 27.09 | 17.45 |
| 4 | April, 2013 | 53.00 | 13/04/13 | 10.15 | 12.87 | 8.32 | 24.29 | 15.69 |
| 5 | May, 2013 | 55.58 | 17/05/13 | 10.33 | 12.61 | 8.16 | 22.68 | 14.67 |
| 6 | June, 2013 | 51.79 | 19/06/13 | 10.42 | 10.87 | 7.08 | 21.00 | 13.68 |
| 7 | July, 2013 | 50.24 | 25/07/13 | 10.38 | 11.13 | 7.26 | 22.14 | 14.45 |
| 8 | August, 2013 | 49.82 | 20/08/13 | 10.25 | 10.96 | 7.15 | 22.00 | 14.36 |
| 9 | September, 2013 | 51.82 | 07/09/13 | 10.00 | 10.79 | 7.02 | 20.82 | 13.56 |
| 10 | October, 2013 | 54.68 | 11/10/13 | 9.33 | 10.78 | 6.99 | 19.72 | 12.79 |
| 11 | November, 2013 | 50.09 | 02/11/13 | 8.75 | 11.95 | 7.70 | 23.85 | 15.37 |
| 12 | December, 2013 | 46.00 | 24/12/13 | 8.50 | 12.41 | 7.99 | 26.99 | 17.37 |

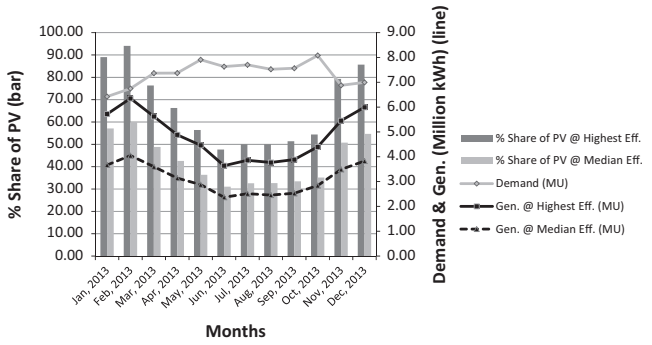


Fig. 14. Demand, generation from PV and % share of demand: Morning Peak (MP).

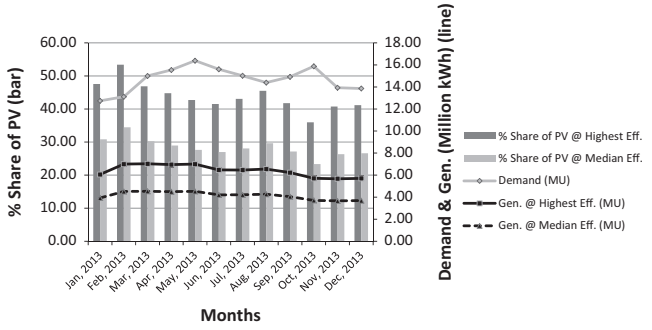


Fig. 15. Demand, generation from PV and % share of demand: Afternoon Partial Peak (APP).

the limits of rated panel efficiency within which the efficiency of the panel, which would actually be used on ground to implement the Mumbai rooftop photovoltaic scenario, would lie. Therefore the most probable band within which the output of the rooftop PV scenario for Mumbai would lie is the one whose boundaries are the outputs produced by the above two solar panel efficiencies. It has been shown in Fig. 10. However, it must be kept in mind that there is a higher cost associated with the higher efficiency panels, and a cost-benefit analysis would help in deciding upon the rated efficiency of the panels actually used for implementation.

## 3. Results for Mumbai rooftop solar PV scenario

This section summarizes the major results for the rooftop solar PV scenario for Mumbai, as described above.

### 3.1. Base case: Fixed tilt @ 19°, median efficiency & highest (commercial) efficiency

It has been found that the total potential for rooftop solar photovoltaic scenario for Mumbai, corresponding to the base case configuration of fixed tilt panels with a tilt of 19°, is 2190 MW. The annual average capacity factor associated with this is 14.8%. The monthly mean capacity factor varies in the range of 13.3–17.2%. The generation possible from this potential capacity varies with the choice of the solar photovoltaic panel efficiency for implementation of the scenario. As discussed in Section 2.3.2, Fig. 7 shows the generation possible (in Million kW h) from the scenario at median rated efficiency and at the highest (commercial) rate efficiency. The intervening band is the most probable band of output in which the generation from the base case rooftop scenario would lie.

Fig. 8 shows the typical daily generation profiles, with median efficiency panels, for the base case rooftop scenario corresponding to the month with highest daily solar irradiance, the month with lowest daily solar irradiance and the annual average daily solar irradiance.

## 4. Comparison with existing power scenario

The estimated output of the rooftop solar photovoltaic scenario, based on the land use data of 2010–11, has been compared with the electricity demand data of MCGM for the year 2013, obtained from Maharashtra State Load Dispatch Center (Combined Daily Reports and Performance Reports, 2013). The total annual demand for 2013 is 18262 Million kWh, whereas for 2010–11 it was 13868 Million kW h (Central Electricity Authority, 2013). The results and the comparison are shown in Fig. 9.

### 4.1. Comparison with daily load profiles

Apart from the above comparison on annual aggregate basis, the average daily rooftop solar PV generation profile for each month has been compared with the typical daily load profiles for those months for the Mumbai region. The daily load profiles have been derived from the Daily System Report generated by the State Load Dispatch Center, Airoli for the Maharashtra State Electricity Transmission Company Ltd. (Combined Daily Reports and Performance Reports, 2013). To decide upon the most typical daily load profile for a month, the load profile of

Table 10
System Peak, Partial Peak and Off-peak: MERC.

| S. no. | Time slot | Classification | TOD tariff (in addition to base tariff) (Rs./kW h) |
|---|---|---|---|
| 1 | 0600–0900 h | Morning Partial Peak (MPP) | 0.00 |
| 2 | 0900–1200 h | Morning Peak (MP) | 0.80 |
| 3 | 1200–1800 h | Afternoon Partial Peak (APP) | 0.00 |
| 4 | 1800–2200 h | Evening Peak (EP) | 1.10 |
| 5 | 2200–0600 h | Off-Peak (OP) | −1.00 |

that day in the month has been taken whose total energy requirement, for the whole day, is closest to the mean daily energy requirement for that month. The results for the month with highest mean daily insolation, February, and for the month with lowest mean daily insolation, October, have been shown in Figs. 10 and 11.

Table 9 summarizes the results for the comparison of typical daily load profiles with the typical solar photovoltaic generation profiles, for each month of the year 2013. The contribution of PV to daily demand has been shown graphically in Fig. 12

### 4.2. Contribution to system peak and partial peak

A better understanding of the contribution of the rooftop solar photovoltaic plan can be made by analyzing the solar generation in perspective of the system peaks over the length of day. As per the Maharashtra Electricity Regulatory Commission (MERC) (Maharashtra State Electricity Distribution Co., Ltd., 2012), Table 10 lists the system peak, partial peak and off-peak times and the corresponding Time-of-Day (TOD) tariffs.

Due to the nature of the solar resource, grid-connected solar photovoltaic, without storage, can provide electrical output during the sunshine hours only. Hence, the rooftop solar photovoltaic plan, as discussed in this paper, can cater to only the first three time slots given in Table 10. The contribution of the rooftop solar photovoltaic plan to the demand during these three time slots, MPP, MP and APP, has been estimated for each month, using the typical days as in Table 9 for representing the respective months; the results for the same have been shown in Fig. 13–15.

## 5. Conclusions

The paper presents a methodology for estimating the rooftop solar photovoltaic potential of a region. It is a hybrid methodology and uses micro–macro synthesis to provide a first order estimate at the macro scale. The use of diverse strategies enables the estimation procedure to overcome the limitations of data availability in public domain for Indian cities. It has the advantage of being simple in nature, and depends only on secondary data available in public-domain.

Public-domain land-use data has been used as the basis for land resource assessment. Geo-spatial analysis of satellite imagery of sample areas yields the BFA Ratios, which are used for extracting, from the plot areas, the total building footprint of the structures suitable for rooftop photovoltaic system installation. A bigger and more diverse sample set would ensure greater accuracy.

Further, the total rooftop area available for photovoltaic installation is extracted from the total Building Footprint Area by the PVA Ratio, which has been estimated from micro-level simulations done in *PVSyst* on sample buildings; the results have also been verified with the corresponding values from literature.

Solar resource assessment depends on the transposition model being used. Having experimental data for DNI, DHI and POA insolation for the place of interest can make the choice of Transposition Model more accurate with respect to the local conditions. The analysis has been presented only for the base case scenario of PV planes' tilt angle fixed at 19°.

Solar photovoltaic devices have been chosen from a comprehensive database, representing the median and the highest (commercial) rated solar cell efficiencies. The results have been appropriately scaled down to reflect the impact of external factors (through PTC and ambient temperatures) and internal heating and losses.

The methodology has been demonstrated for the Indian city of Mumbai. The results show a rooftop solar photovoltaic potential of 2190 MW for the city, with median efficiency panels. The annual average capacity factor is found to be 14.8%. The comparison between sample daily load profiles of the city and the typical expected

Table A.1
Inputs for the Analysis.

| S. no. | Name | Source |
|---|---|---|
| 1 | Existing Land Use (ELU) data for various Categories and Sub-categories | Existing Land Use Survey Data by MCGM |
| 2 | Satellite Imagery samples from the region of interest | Google Earth |
| 3 | Photovoltaic-Available Roof Area (PVA) Ratios | Literature Review + *PVSyst* Simulations |
| 4 | Performance Metrics of various Transposition Models | Literature Review |
| 5 | Albedo, PV Plane Orientation, PV Plane Tilt Angle | Conventional Values |
| 6 | Solar Insolation Data (DNI and DHI) for Mumbai | Climate Design Data 2009 ASHRAE Handbook |
| 7 | Ambient Temperature Data for Mumbai | Climate Design Data 2009 ASHRAE Handbook |
| 8 | Cut-in and Cut-off Solar Elevation Angles | *PVSyst* Simulations |
| 9 | Highest (Commercial) and Median PV panel efficiencies | SRoeCo Solar: Solar Panel Database |
| 10 | Highest and Median PTC values | SRoeCo Solar: Solar Panel Database |
| 11 | Annual Electrical Energy Consumption and Requirement Data for Mumbai | Central Electricity Authority Report |
| 12 | Monthly Energy Consumption statistics for Mumbai | Monthly Reports by Maharashtra State Load Dispatch Center |
| 13 | Typical Daily Load Profiles of Mumbai for Sample Days | Daily System Report by Maharashtra State Load Dispatch Center |
| 14 | Population of Mumbai (MCGM) and Greater Mumbai Urban Agglomeration | 2011 Census of India Data |

photovoltaic generation profiles shows that the rooftop solar photovoltaic plan has the potential to provide 12.8–20% of the daily demand, during different months, with median efficiency panels; with highest (commercial) efficiency panels this range goes up to 19.7–31.1%. The plan can meet 31% to 60% of the morning peak demand (0900–1200 h) during different months with median efficiency panels; and 47.7–94.1% of the morning peak demand with highest (commercial) efficiency panels.

The methodology can be extended to any city. Based on the secondary land-use data and satellite image analysis first-order estimates can be made. Thus it provides a simple tool for generating estimates which can aid in policy decisions for large scale implementation of rooftop solar photovoltaic based renewable scenarios.

## Appendix A

To summarize, the complete methodology described above uses the following parameters, listed in Table A.1, as inputs. Also listed in the table are the sources from which the values of these parameters have been chosen.

## References


American Society of Heating, Refrigerating and Air Conditioning Engineers, 2009. Climate Design Data 2009 ASHRAE Handbook.

Bergamasco, L., Asinari, P., 2011. Scalable methodology for the photovoltaic solar energy potential assessment based on available roof surface area: application to Piedmont Region (Italy). Sol. Energy 85 (5), 1041–1055.

Bilbao, J., De Miguel, A., Ayuso, A., Franco, J.A., 2003. Iso-radiation maps for tilted surfaces in the Castile and Leon region, Spain. Energy Convers. Manage. 44 (9), 1575–1588.

Central Electricity Authority, 2013. 18th Electric Power Survey (EPS) of India (volume-II).

Combined Daily Reports and System Performance Reports, Maharashtra State Load Dispatch Centre, 2013 <http://mahasldc.in/reports> (05.05.14).

Demain, C., Journée, M., Bertrand, C., 2013. Evaluation of different models to estimate the global solar radiation on inclined surfaces. Renew. Energy 50, 710–721.

Evseev, E.G., Kudish, A.I., 2009. The assessment of different models to predict the global solar radiation on a surface tilted to the south. Sol. Energy 83 (3), 377–388.

Existing Land Use Survey for Development Plan for Greater Mumbai (2014–2034), 2013 http://www.mcgm.gov.in/irj/portal/anonymous/qlELUSurveyData (21.09.13).

Greenpeace India, 2013. Rooftop Revolution: Unleashing Delhi's Solar Potential.

Gueymard, C.A., 2009. Direct and indirect uncertainties in the prediction of tilted irradiance for solar engineering applications. Sol. Energy 83 (3), 432–444.

India Solar Resource Maps, Solar Energy Centre, Ministry of New and Renewable Energy, Government of India, 2013 <http://mnre.gov.in/sec/solar-assmnt.htm> (17.12.13).

International Energy Agency, 2002. Potential for Building Integrated Photovoltaics, Report IEA–PVPS T7-4.

Izquierdo, S., Rodrigues, M., Fueyo, N., 2008. A method for estimating the geographical distribution of the available roof surface area for large-scale photovoltaic energy-potential evaluations. Sol. Energy 82 (10), 929–939.

Jakubiec, J.A., Reinhart, C.F., 2012. Towards validated urban photovoltaic potential and solar radiation maps based on LiDAR measurements, GIS data, and hourly DAYSIM simulations. In: Proceedings of SimBuild, Madison, Wisconsin, pp. 1–10.

Kambezidis, H.D., Psiloglou, B.E., Gueymard, C., 1994. Measurements and models for total solar irradiance on inclined surface in Athens, Greece. Sol. Energy 53 (2), 177–185.

Karteris, M., Slini, T., Papadopoulos, A.M., 2013. Urban solar energy potential in Greece: a statistical calculation model of suitable built roof areas for photovoltaics. Energy Build. 62, 459–468.

Liu, B.Y., Jordan, R.C., 1960. The interrelationship and characteristic distribution of direct, diffuse and total solar radiation. Sol. Energy 4 (3), 1–19.

Maharashtra State Electricity Distribution Co., Ltd., 2012. MERC Order for Tariff determination of FY 2012–13.

Ministry of New & Renewable Energy, Government of India, 2012. Jawaharlal Nehru National Solar Mission: Phase II – Policy Document.

Montavon, M., Scartezzini, J.L., Compagnon, R., 2004. Solar energy utilisation potential of three different Swiss urban sites. Energie und Umweltforschung im Bauwesen, Zurich, pp. 503–510.

Mumbai (Greater Mumbai) Metropolitan Urban Region Population 2011 Census, 2011 <http://www.census2011.co.in/census/metropolitan/305-mumbai.html> (17.12.13).

Notton, G., Poggi, P., Cristofari, C., 2006. Predicting hourly solar irradiations on inclined surfaces based on the horizontal measurements: performances of the association of well-known mathematical models. Energy Convers. Manage. 47 (13), 1816–1829.

Ordóñez, J., Jadraque, E., Alegre, J., Martínez, G., 2010. Analysis of the photovoltaic solar energy capacity of residential rooftops in Andalusia (Spain). Renew. Sustain. Energy Rev. 14 (7), 2122–2130.

Padovan, A., Del Col, D., 2010. Measurement and modeling of solar irradiance components on horizontal and tilted planes. Sol. Energy 84 (12), 2068–2084.

Pillai, I.R., Banerjee, R., 2007. Methodology for estimation of potential for solar water heating in a target area. Sol. Energy 81 (2), 162–172.

Ross Jr., R.G., 1980. Flat-plate photovoltaic array design optimization. 14th Photovolt. Special. Conf. 1, 1126–1132.

Ross, Jr., R.G., Smokler, M.I., 1986. Flat-plate solar array project: final report, vol. 6, Engineering Sciences and Reliability (No. DOE/JPL-1012-125-Vol. 6). Jet Propulsion Lab., Pasadena, CA, USA.

Scartezzini, J.L., Montavon, M., Compagnon, R., 2002. Computer evaluation of the solar energy potential in an urban environment. Eurosun 2002 Conf.

SRoeCo Solar: Solar Panel Comparison Table, 2014. <http://sroeco.com/solar/table/> (Oct. 08, 2013–Jan 29, 2014).

Theodoridou, I., Karteris, M., Mallinis, G., Papadopoulos, A.M., Hegger, M., 2012. Assessment of retrofitting measures and solar systems' potential in urban areas using geographical information systems: application to a mediterranean city. Renew. Sustain. Energy Rev. 16 (8), 6239–6261.

Wiginton, L.K., Nguyen, H.T., Pearce, J.M., 2010. Quantifying rooftop solar photovoltaic potential for regional renewable energy policy. Comput. Environ. Urban Syst. 34 (4), 345–357.

Yue, C.D., Huang, G.R., 2011. An evaluation of domestic solar energy potential in Taiwan incorporating land use analysis. Energy Policy 39 (12), 7988–8002.